Environmental Science & Technology

Article

pubs.acs.org/est

Abiotic and Biotic Factors That Influence the Bioavailability of Gold Nanoparticles to Aquatic Macrophytes

J. Brad Glenn*[,†,‡] and Stephen J. Klaine[†,§]

[†]Clemson Institute of Environmental Toxicology, Clemson University, Clemson, South Carolina, 29634 United States

[‡]Graduate Program of Environmental Toxicology, Clemson University, Clemson, South Carolina, 29634 United States

[§]Department of Biological Sciences, Clemson University, Clemson, South Carolina, 29634 United States

ABSTRACT: This research identified and characterized factors that influenced nanomaterial bioavailability to three aquatic plants: *Azolla caroliniana* Willd, *Egeria densa* Planch., and *Myriophyllum simulans* Orch. Plants were exposed to 4-, 18-, and 30-nm gold nanoparticles. Uptake was influenced by nanoparticle size, the presence of roots on the plant, and dissolved organic carbon in the media. Statistical analysis of the data also revealed that particle uptake was influenced by a 4-way (plant species, plant roots, particle size, and dissolved organic carbon) interaction suggesting nanoparticle bioavailability was a complex result of multiple parameters. Size and species dependent absorption was observed that was dependent on the presence of roots and nanoparticle size. The presence of dissolved organic carbon was found to associate with 4- and 18-nm gold nanoparticles in suspension and form a nanoparticle/organic matter complex that resulted in (1) minimized particle aggregation and (2) a decrease of nanoparticle absorption by the aquatic plants. The same effect was not observed with the 30-nm nanoparticle treatment. These results indicate that multiple factors, both biotic and abiotic, must be taken into account when predicting bioavailability of nanomaterials to aquatic plants.

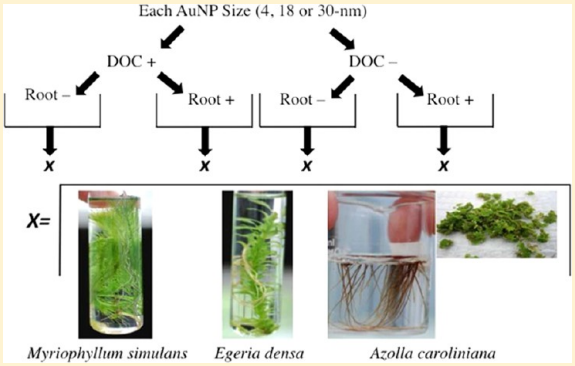

INTRODUCTION

The consequences of environmental release of nanomaterials (NMs) are uncertain. The uncertainty regarding the fate and effects of NMs in the environment has been identified in several recent papers as critical knowledge gaps that prevent the quantitative assessment of environmental risk and limit the nanomaterials management in aquatic ecosystems.[1−9] Studies focused on the release of NMs in the environment range from modeling exposure through life cycle assessment to predict surface water concentrations[10,11] to characterizing the effects of NMs on crop plants and terrestrial plant health such as wheat, squash, pumpkin, tobacco, and rice.[12−17] At this time, detailed studies of the interactions of NMs with aquatic plants are limited.[18,19] Since plants represent a large interface that interacts closely between the environment and biosphere in both terrestrial and aquatic systems, this interface is in need of further investigation with regards to NMs and their distribution, fate, and potential effects.

Recent review papers by Rico et al.[20] and Miralles et al.[21] have inventoried the interactions that NMs have with terrestrial plants. The common end points for measuring plant−nanoparticle interactions include germination and root/shoot elongation. While these measurements provide valuable data sets, additional studies that address more in-depth modes of action are needed. From Rico et al.,[20] it is clear that a paucity of information exists about NM interactions with plants and factors that influence their bioavailability. These factors include NM size and shape, route of uptake, bulk NM composition, and surface chemistry. Miralles et al.[21] advances the need for more information and understanding on how NMs are taken up and transported within plants, including bioavailability.

Terrestrial plants may come in contact with NMs through atmospheric deposition, improper disposal of NM containing compounds, and from land applied sewage sludge, a known sink for NMs.[16,22,23] Through storm events, runoff, erosion, and improper or the lack of best management practices, the aquatic environment will then serve as sinks for NMs. Although much literature is focused on the impact of NMs on terrestrial crop species, some of the results obtained to date are relevant to aquatic plants. Many similarities exist between aquatic and terrestrial plant physiology, such as vascular systems, photosynthesis structures, and plant organ systems (roots, leaves). A difference however is that aquatic macrophytes can absorb nutrients from both roots and leaves.[24] This difference in nutrient acquisition warrants further investigation into parameters that influence absorption of NM in aquatic vascular plants, as roots may not be the only site of NM absorption. Studies have shown NMs are capable of penetrating into the roots of many different species of plants, typically limited to

Received: May 7, 2013
Revised: August 3, 2013
Accepted: August 15, 2013
Published: August 15, 2013

 © 2013 American Chemical Society

pores present in the microfibril network structure of the cell wall. These pores (gaps in microfibril layers) limit the diameter of structures that are capable of penetrating through to the cell membrane. Typical pore structures of higher plants have been reported to range from 3-nm up to reported values of near 20-nm, showing differences among plant species.[16,20,21,25,26] Contradicting this exclusion mechanism, however, studies have published absorption of larger NMs including carbon nanotubes and AuNPs that are larger than the pore structures present.[20,26] This evidence suggests another route of absorption, through wounding of tissue, creation of new pore structures, stomata absorption, or even active transport across cell membranes.[20,21,27] As progress is made in understanding NM interactions with terrestrial plants, additional studies are needed with respect to aquatic plants. Probable mechanisms of uptake, translocation, and toxicity are scarce to nonexistent. Further, research into biotic and abiotic factors that influence NM bioavailability to aquatic plants is also needed.

Because aquatic plants are often fully submerged, water quality parameters become critical in understanding bioavailability of NMs to aquatic macrophytes. Water hardness plays a well-known role in aggregation of NMs. Also, pH can dictate speciation of NMs and aggregation state. The presence of a chelator such as natural organic matter (NOM) can also influence bioavailability. Natural organic matter may vary in concentrations and chemical composition but is considered ubiquitous in water bodies.[19] Natural organic matter can influence the stability, charge, and surface chemistry of NMs.[28−30] Stankus et al.[28] found very similar surface properties between AuNPs with different surface chemistries, indicating that AuNP surface chemistry no longer is the driving force of the particles stability when in the presence of NOM. Diegoli et al.[29] proposed NOM replaces the citrate surface chemistry of the AuNPs, stabilizing the AuNPs from aggregation. This replacement of surface chemistry resulted in more stable suspensions of particles, which did not aggregate even in extreme pH ranges. Nanoparticle and NOM interactions do vary however between NOM isolates, and the higher molecular weight humic acids were found to give the citrate coated AuNPs the greatest ability to avoid destabilization.[30] Natural organic matter consists of humic and fulvic acids, both known to have the ability to chelate metal ions and organic pesticides[31−33] and stabilize AuNPs.[28−30] This interaction of NOM with AuNPs is hypothesized to reduce the absorption of AuNPs by aquatic plants due to the AuNPs binding with the NOM and forming a larger, more stable complex.

In order to better address NM bioavailability to aquatic plants, biotic and abiotic factors were investigated. The effect of plant species, root presence, natural organic matter, and nanoparticle size were studied using a factorial experimental design to capture each effect and interactions between effects. Gold nanoparticles (AuNPs) served as a model NM for tracking within the aquatic plant. Due to their ease of synthesis in various sizes, stability in suspension, and ability to be visualized, AuNPs represent a good model NM for tracking studies.[34−37] Further, AuNPs are useful in bioconcentration studies with plants due to the minimal chance of toxicity.[18,38] The interactions NMs have with aquatic plants is important in understanding potential for NM fate, transfer, and possible escape from the aquatic ecosystem.

■ EXPERIMENTAL SECTION

Nanoparticle Synthesis and Characterization. Four, 18, and 30 nanometer (nm) gold nanoparticle spheres (AuNPs) were synthesized following the Turkevich and related Frens method[37,39,40] at the Clemson University Institute of Environmental Toxicology (CU-ENTOX). The 4-nm AuNPs were synthesized by combining 0.5 mL of 0.01M chloroauric acid with 19 mL of Milli-Q water, and 0.5 mL of 0.01M sodium citrate tribasic dihydrate. After, 0.6 mL of 0.1M sodium borohydride was added to reduce the chloroauric acid completing the process. The 18-nm AuNPs were synthesized by combining 2.5 mL of 0.01M chloroauric acid with 97.5 mL of Milli-Q water. The solution was brought to a boil, and 3 mL of 1% by weight sodium citrate reduced the chloroauric acid, forming the AuNPs. Lastly, for the 30-nm AuNPs, 2.5 mL of 0.01 M-chloroauric acid was combined with 100 mL of Milli-Q water. The solution was then boiled, and 10 mL of 1% by weight sodium citrate solution was added to reduce the chloroauric acid.

Gold nanoparticle size and morphology characterization was performed with transmission electron microscopy (Hitachi H-7600) in both stock and exposure media at the Clemson Microscope Facility. Electrophoretic mobility measurements were measured on a Malvern Zetasizer Nano of stock and treatment suspensions.

Nanoparticle Suspensions. Nanoparticle suspensions were made in 0.45 μm filtered well water (PALL type A/E Glass fiber filters). For the DOC treatments, Suwannee River aquatic reference NOM (1R101N) was purchased from the International Humic Substances Society, IHSS. NOM was added to filtered well water (0.45-μm) at the nominal concentration of 5 mg/L, stirred overnight, and then filtered with a 0.45-μm, glass fiber filter (PALL type A/E) to capture the dissolved organic carbon (DOC) fraction. After filtration, organic carbon content (mg C/L) was analyzed using a Shimadzu total organic carbon analyzer.

Plant Species. Aquatic macrophytes used were cultured in a double-layer, polyethylene-covered greenhouse in Pendleton, SC (25 ± 2 °C, 14:10 h light/dark). All plants selected for this study appeared healthy and had no visible periphyton growth. Plant cultures were not axenic. Plants were rinsed vigorously with distilled water before experimental use. Experiments were conducted in the greenhouse during July and August 2012.

Microscopy. Gold nanoparticle suspension samples were captured on 200-mesh, carbon Formvar copper grids (type FCF200-Cu). The Hitachi 7600 (120kv) and Hitachi 9500 (300 kV) transmission electron microscopes (TEM) were used to image nanomaterials in bright field micrographs. The Hitachi HD-2000 scanning transmission electron microscope (STEM) was used to image dark field micrographs (Electron Microscope Facility, Clemson University).

Experimental Design. The experimental setup was a 24-h static exposure with a 2 × 2 × 3 × 3 randomized complete factorial design. Factors included plant species (*M. simulans*, *E. densa*, and *A. caroliniana*), plant roots (R+, present or R−, absent), particle size (4-, 18- or 30-nm AuNPs) and SR-NOM (DOC+, present, or DOC−, absent) for a total of 36 treatments. All roots were removed at the plant base via razor blade prior to exposure in the R− treatment. Each treatment combination was performed in triplicate. Gold nanoparticle suspensions were made at a nominal concen-

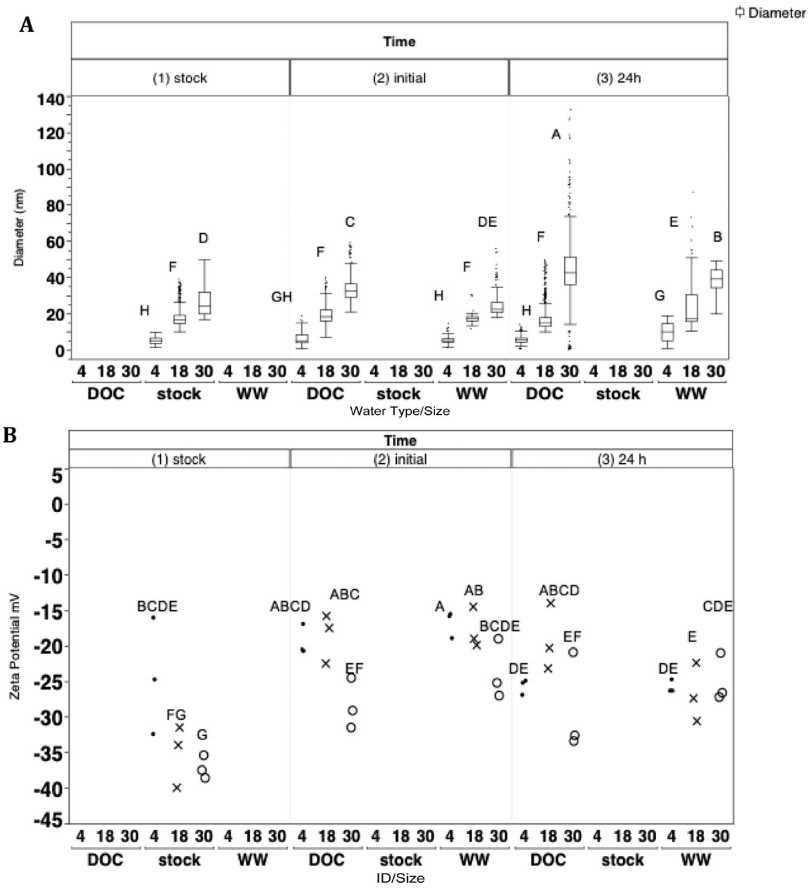

Figure 1. Characterization graphs of citrate gold nanoparticles. (A) Box graphs of gold nanoparticle core diameter in nanometers overlaid with water treatment and sampling time. n = 250−1200 particles per treatment. Core diameter measured with transmission electron microscopy (Hitachi H-7600). B) Electrophoretic mobility measurements of gold nanoparticle treatments overlaid with water treatments and sampling time. n = 3. DOC = contains dissolved organic carbon, WW = well water, stock = undiluted nanoparticle stock suspension, initial = time 0 suspension, and 24 h = 24 h post suspension. Statistics defined in Data Analysis section.

tration of 250 μg Au/L and then subdivided for each treatment replicate.

Myriophyllum simulans and *Egeria densa* were exposed in 70 mL glass test tubes. *Azolla caroliniana* was exposed in 30 mL glass beakers. Before exposure, glassware was acetone and acid washed (10% nitric). After harvest, plants were vigorously rinsed in distilled water by submerging 10 times. The final dry tissue weight (g) was recorded after 24 h of drying at 60 °C in a drying oven.

Gold Analysis. Tissue digestion was performed on the basis of a modified method from Anderson et al.[41] Dried tissue was transferred to 20 mL cleaned ceramic crucibles and was heated to 530 °C for 14 h in a muffle furnace to ash and facilitate breakdown of plant cellulose and lignin components. Crucibles were cleaned with *aqua regia*. Once cooled, tissue was digested with *aqua regia* (1:3 nitric to hydrochloric trace grade acids) and then diluted to achieve 5% volume acid for analysis using ICP-MS (ThermoScientific Xseries2). Water samples were acidified to achieve 5% volume acid using *aqua regia*.

Data Analysis. Analysis of variance indicated a significant difference in main effects for gold nanoparticle size distribution and electrophoretic mobility. Due to large sample size (n = 250−1200) in the particle size analysis, Tukey's HSD was used to separate main effects revealing significant differences between treatments. Students-t test was used to separate main effects for gold nanoparticle electrophoretic mobility measurements, n = 3. A full factorial, standard least-squares analysis of main effects (plant species, plant roots, particle size, and SR-NOM) was conducted using JMP v10.0 (SAS Institute Inc., Cary, NC). Interactions of main effects were significant ($p < 0.001$) and were separated using students-t test ($\alpha = 0.05$). The interaction profiler was used to characterize interactions of main effects.

RESULTS AND DISCUSSION

Gold Nanoparticle Characterization. Each size of the gold nanoparticles in stock and treatment suspensions (initial and 24 h time points) was characterized for size by transmission electron microscopy (TEM) and stability with zeta potential. The same samples were used in each characterization analysis. Gold concentration remained consistent throughout the exposures, at 248.9 ± 11.0 μg Au/L. Dissolved organic carbon for each treatment was normalized to carbon, C content. Well water only treatments (DOC−) had 0.1 ± 0.02 mg C/L, and well water with DOC (DOC+) had 2.0 ± 0.4 mg C/L. The well water used in this study had a pH of 6.8, hardness of 100 mg/L $CaCO_3$, and alkalinity of 80 mg/L $CaCO_3$. The nominal AuNP sizes of 4-, 18-, and 30-nm were determined from the stock suspensions (5.2 ± 2.0-nm, 18.1 ± 5.6-nm, and 27.0 ± 8.0-nm, respectively (n = 250−1200 particles)). Figure 1 shows all of the data points gathered for AuNP characterization, and Table 1 summarizes these characterization results. For all AuNPs, a

Table 1. Characterization Averages for Gold Nanoparticles in Each Exposure Treatment

sample ID	ζ, suspension[a] (mV) initial /(24 h)	TEM diameter[b] (nm) initial /(24 h)
	Stock	
4-nm	−24.4 ± 8.2/(n/a)	5.2 ± 2.0/(n/a)
18-nm	−35.2 ± 4.4/(n/a)	18.1 ± 5.6/(n/a)
30-nm	−37.2 ± 1.6/(n/a)	27.0 ± 8.0/(n/a)
	Well Water	
4-nm	−16.7 ± 1.8/(−25.8 ± 0.9)	8.0 ± 6.0/(10.0 ± 5.0)
18-nm	−17.8 ± 2.9/(−26.8 ± 4.1)	17.5 ± 2.4/(23.3 ± 12.5)
30-nm	−23.7 ± 4.2/(−24.9 ± 3.4)	25.0 ± 7.0/(39.1 ± 8.0)
	Well Water/DOC	
4-nm	−19.4 ± 2.1/(−25.7 ± 1.1)	6.6 ± 3.6/(5.6 ± 1.8)
18-nm	−18.5 ± 3.5/(−19.2 ± 4.7)	20.2 ± 6.6/(18.4 ± 8.4)
30-nm	−28.4 ± 3.6/(−29.0 ± 7.0)	34.1 ± 7.8/(42.3 ± 8.3)

[a]Zeta $n = 3$ (mV ± std dev), pH 7.1. [b]$n = 250–1200$ particles.

loss in stability was observed in treatment suspensions. The 4-nm AuNPs stock suspension had an electrophoretic mobility of −24.4 ± 8.2 mV, suggesting these particles are moderately unstable. The measurement is likely due to the high ionic strength, as these particles were not purified to remove excess sodium that results from the addition of sodium borohydride. In the 4-nm AuNP well water treatment, the zeta potential decreases to −16.7 ± 1.8 mV, which can be explained by the increase in water hardness of 100 mg/L as $CaCO_3$. After 24 h however, the zeta potential indicates a gain of stability to −25.8 ± 0.9 mV. The increase in the 4-nm AuNP treatment occurs simultaneously with a gain in particle size mean from initial 8.0 ± 6.0-nm to 24 h size of 10.0 ± 5.0-nm. This size increase is mitigated with the addition of DOC. In the well water with DOC treatment, the initial zeta potential is −19.4 ± 2.1 mV shifting to −25.7 ± 1.1 mV after 24 h. Particle size in the DOC + treatment showed reduced particle aggregation with initial size being 6.6 ± 3.6-nm to 5.2 ± 1.8-nm after 24 h in suspension. Compared to the 24 h values for the well water, DOC− treatment (10.0 ± 5.0-nm) and well water DOC+ treatment (5.2 ± 1.8-nm) indicates a potential effect DOC has in reducing particle aggregation.

The 18-nm AuNPs stock suspension was moderately stable (−35.2 ± 4.4 mV) whereas the well water treatment suspensions showed a reduction in initial AuNP stability (−17.8 ± 2.9 mV) that shifted to to −26.8 ± 4.1 mV after 24 h. This shift in stability correlated with an increase average particle size, initial 17.5 ± 2.4-nm to 24h 23.3 ± 12.5-nm, indicating the onset of aggregation in the well water treatment. The addition of DOC did not have an effect on particle stability (initial −18.5 ± 3.5 mV to 24 h −19.2 ± 4.7 mV); however, when comparing the mean core diameter of the 18-nm AuNPs in both the well water treatment (23.3 ± 12.5-nm) and DOC well water treatment (18.4 ± 8.4-nm), the core diameter becomes more similar to that of the stock suspension (18.1 ± 5.6-nm). When comparing these results to the 18-nm well water only treatment, it indicates DOC had an effect mitigating particle aggregation and polydispersity.

The 30-nm AuNP stock suspension had the highest stability of all particles (−37.2 ± 1.6 mV). When well water treatment suspensions were made, the zeta potential showed an initial decline to −23.7 ± 4.2 mV and then after 24 h remained the same at −24.9 ± 3.4 mV. With the addition of DOC, no change was observed in particle stability. Comparing particle size for the well water treatment, the onset of aggregation was observed (initial 25.0 ± 7.0-nm to 24 h of 39.1 ± 8.0-nm). With the addition of DOC, similar results were observed, where the onset of particle aggregation was still observed in the well water DOC treatment (initial 34.1 ± 7.8-nm to 24 h 42.3 ± 8.3-nm). In this treatment, the addition of DOC did not reduce the average particle core diameter.

Gold Nanoparticles and Aquatic Macrophytes. It has been documented that the absorption of AuNPs by aquatic plants is AuNP size and plant species dependent.[18] This is supported by several studies that found that NMs absorption by terrestrial plants are specific to NM characteristics, as well as the plant species.[16,26,42−44] However, the current mechanisms

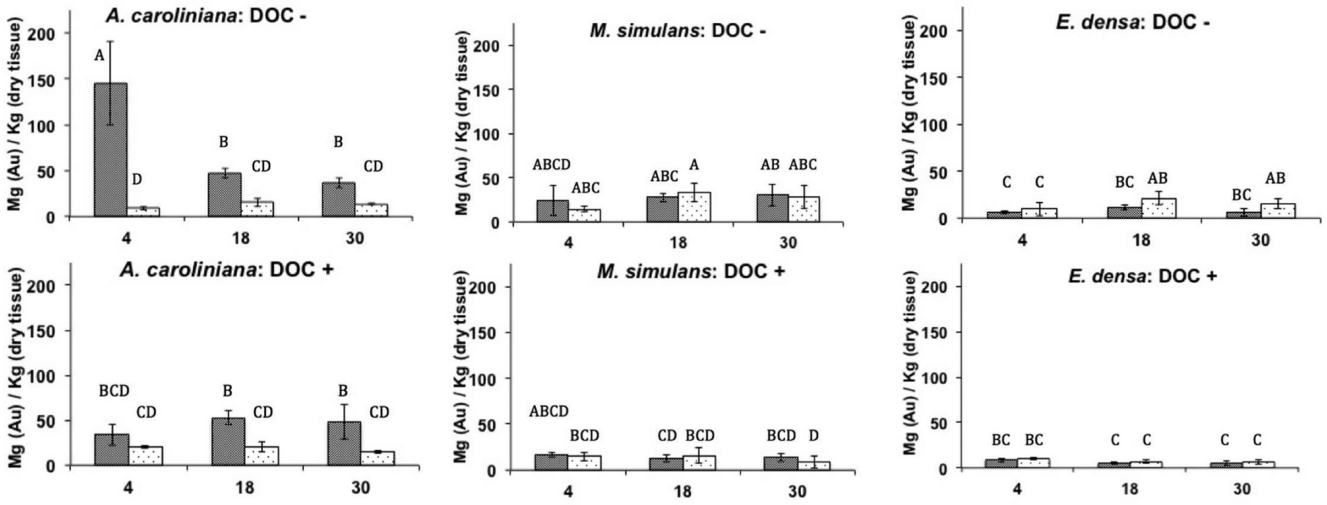

Figure 2. Tissue concentration graphs of complete factorial design aquatic plant study. Species are indicated by graph heading, and DOC− (top row) indicates exposure suspension in only well water. The DOC+ (bottom row) indicates the addition of Suwannee river dissolved organic carbon. *X*-axis shows the gold nanoparticle sizes in nanometers for each treatment. Gray bars indicate the presence of roots, while white bars indicate roots removed in each treatment. Error bars indicate standard deviation of the mean ($n = 3$). Statistical analysis letters are only comparable between same plant species graphs.

of NMs absorption and translocation in plants are ultimately unknown.[16,19−21,43] In order to better address factors that influence the absorption of AuNPs from suspension to aquatic plants, 2 biotic and 2 abiotic factors were investigated. These factors included three plant species, roots (R+, present, or R−, absent), DOC (DOC+, presence, or DOC−, absence), and AuNPs in three sizes (4-, 18-, and 30-nms).

The three specific plant species utilized each had unique characteristics. *Azolla caroliniana* is a free-floating aquatic fern with scale like leaves. It has many slender roots that protrude from the floating leaf bottoms and reside in the water column with an average length of 4−6 cm. These roots contain root hair structures that increase the surface area of the roots in contact with the water column. Stomata are also present on the leaf surface.[45] Because *A. caroliniana* is free floating, it has a transpiration stream present. *Myriophyllum simulans* is fully submerged and can be rooted in the sediment or free floating in the water column. It may or may not have roots present. The leaf structure is needle-like, and leaves grow in whorls around each node. *Egeria densa* is also fully submerged. This species has broad whorls of 4 leaves around each node. *Egeria densa* is either rooted into the sediment or free floating. The root structure of *E. densa* may or may not be present. Roots propagate from a root crown node, typically one or two roots at a time.[46] These roots are adventitious, which develop to anchor the plant into the sediment.

Factors That Affect Bioavailability of AuNPs. Figure 2 shows each species broken down into the individual treatment factors of root presence (R+ or R−), DOC (DOC− or DOC +), AuNP size (4-, 18-, and 30-nms), and species (*A. caroliniana*, *M. simulans*, and *E. densa*). Four way interactions among factors were found significant ($p > 0.0026$) indicating that treatment combinations had an effect on tissue gold concentrations. Overall, interpreting data by species indicates that *Azolla caroliniana* was most sensitive to tissue gold concentration change by treatment factors, which will be discussed later. The results further support that AuNPs absorption by aquatic plants is species dependent, as shown by previous research.[18]

These results suggest that tissue concentrations observed in *E. densa* were due to surface adsorption only. They are supported by previous research indicating that *E. densa* does not absorb 4- or 18-nm AuNPs from suspension.[18] Breaking *E. densa* results down by treatment, the DOC− and R+ treatments for 4-, 18-, and 30-nm AuNPs resulted in statistically similar tissue concentrations of 6.3 ± 1.4, 11.3 ± 2.4, and 6.3 ± 4.2 mg Au/kg, respectively. The DOC− and R+ treatment also indicates that root or shoot absorption is not a driver of AuNP uptake, since statistically similar results were seen in the DOC− and R− treatment, with the 4-, 18-, and 30-nm AuNPs tissue concentrations being 10.0 ± 7.2, 21.1 ± 7.0, and 15.1 ± 5.4 mg Au/kg, respectively. Also, there is no AuNP size dependence observed in treatment tissue concentrations, supporting only the surface adsorption of AuNPs. This was also observed in the DOC+ treatment whereas no significant effect of roots was found to correlate with tissue concentrations.

For the DOC+ and R+ treatment, tissue gold concentrations observed were 8.6 ± 1.9, 5.3 ± 1.7, and 5.1 ± 2.8 mg Au/kg for 4-, 18-, and 30-nm, respectively, and the R− resulted in statistically similar tissue gold concentrations of 10.2 ± 1.5, 7.0 ± 2.3, and 6.6 ± 2.5 mg Au/kg for 4-, 18-, and 30-nm, respectively. Comparing the DOC+ and DOC− treatment for *E. densa*, a general trend indicates a decline of tissue gold concentration with the addition of DOC, although it is not significant for all AuNP sizes.

Results for *Myriophyllum simulans* indicate higher gold tissue concentrations than *E. densa* for each AuNP size range. For *M. simulans*, no significant differences in tissue gold concentrations were observed across AuNP sizes. Breaking down tissue gold concentration results by treatment, the DOC− and R+ treatment observed tissue concentrations for 4-, 18-, and 30-nm AuNPs of 23.9 ± 16.8, 27.8 ± 5.0, and 30.3 ± 12.2 mg Au/kg compared to the DOC− and R− treatment for the same sizes with tissue concentrations of 14.5 ± 2.9, 33.4 ± 11.0, and 28.3 ± 13.0 mg Au/kg, respectively. Comparing the tissue gold concentrations for the R+ and R− treatments for the DOC− treatment above also indicated that shoots are not a significant driver of AuNP absorption.

Tissue concentrations for the DOC+ and R+ treatment observed for the 4-, 18-, and 30-nm AuNPs were 16.8 ± 2.3, 12.9 ± 3.8, and 14.0 ± 4.5 mg Au/kg, respectively, compared to the tissue gold concentrations for DOC+ and R− treatment of 14.8 ± 4.6, 15.6 ± 8.3, and 8.7 ± 7.0 mg Au/kg for the same size AuNPs. Although not significant for all AuNP sizes, the addition of DOC to the treatments indicates a general decline in gold tissue concentration.

Azolla caroliniana results indicate DOC and roots play an important role in gold tissue concentrations. For the 4-nm AuNP and DOC− treatment, the removal of roots (R−) resulted in the largest decrease in tissue concentration from the R+ treatment, 145.5 ± 45.5 mg Au/kg to 9.0 ± 1.5 mg Au/kg, indicating roots are the primary absorption mechanism of 4-nm AuNPs. When only *A. caroliniana* shoots were exposed to each size AuNP in the DOC− treatment, tissue concentrations do not significantly change, representing non-AuNP size specific adsorption to the leaf surfaces (9.0 ± 1.5, 15.8 ± 4.7, and 13.8 ± 1.0 mg Au/kg for 4-, 18-, and 30-nm AuNPs). For both the 18- and 30-nm AuNPs in the DOC− treatment, a decrease in tissue concentration can be observed with the absence of roots. The R+ treatment resulted in concentrations of 47.1 ± 5.3 and 36.4 ± 5.3 mg Au/kg that were significantly higher than the R− treatment (15.8 ± 4.7 and 13.8 ± 1.0 mg Au/kg) for 18- and 30-nm AuNPs, respectively.

Comparing the DOC− and DOC+ graphs for *A. caroliniana*, the addition of DOC resulted in a decreased tissue concentration, even with roots present. In the 4-nm AuNP, DOC+, and R+ treatment for *A. caroliniana*, the addition of DOC resulted in a decreased tissue concentration from the DOC− treatment, 145.5 ± 45.4 to 33.8 ± 11.4 mg Au/kg, respectively. In the DOC+ and R+ treatment, AuNP size effect on tissue concentration is mitigated by the presence of DOC, as tissue gold concentrations are not significantly different for the DOC+ and R+ treatment (33.8 ± 11.3, 52.4 ± 7.5, 48.1 ± 19.1 mg Au/kg) for the 4-, 18-, and 30-nm treatments, respectively. In the DOC+ and R− treatment, a further decrease in tissue concentration occurs with the removal of roots to 20.3 ± 1.0, 20.3 ± 6, and 14.8 ± 2.0 mg Au/kg for the 4-, 18-, and 30-nm treatments. This difference in tissue gold concentration is most likely due to the decrease in adsorption sites for the AuNPs to attach. Comparing only the 18- and 30-nm AuNPs in the DOC− to the DOC+ treatment, DOC does not have a significant effect on reducing tissue gold concentrations. For DOC−, tissue gold concentrations are 47.5 ± 5.3 and 36.4 ± 5.3 mg Au/kg, and DOC+ tissue gold concentrations are 52.4 ± 7.5 and 48.1 ± 19.0 mg Au/kg, for the 18- and 30-nm AuNPs, respectively. This indicates that the presence of DOC

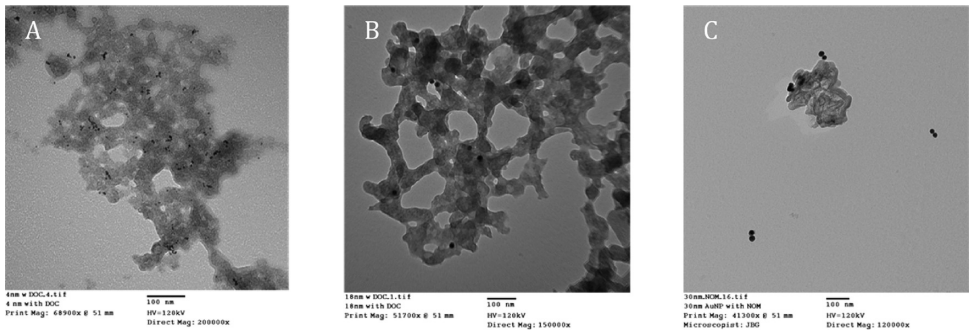

Figure 3. Transmission electron micrographs of gold nanoparticles associated with Suwannee River dissolved organic carbon. (A) Represents 4-nm gold nanoparticles. (B) Represents 18-nm gold nanoparticles. (C) Represents 30-nm gold nanoparticles. Scale bar represents 100-nm.

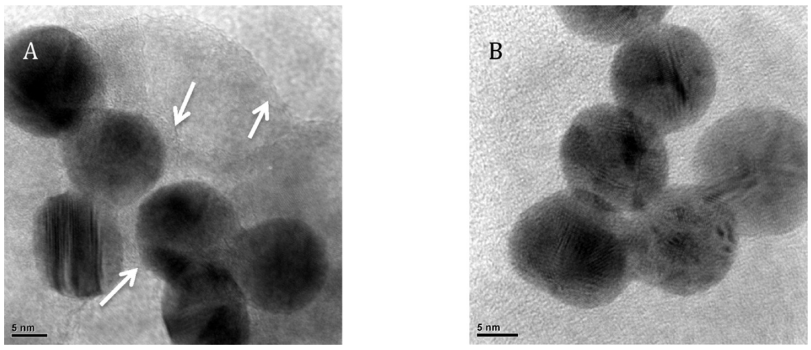

Figure 4. High-resolution transmission electron micrograph of 18-nm gold nanoparticles. (A) Shows 18-nm gold nanoparticles associated with Suwannee River dissolved organic carbon. (B) Shows 18-nm gold nanoparticle stock suspension without any dissolved organic carbon present. Note the white arrows indicate the close association of dissolved organic carbon with the particle core. Scale bar = 5-nm.

and the presence of roots have the largest effect on the 4-nm AuNPs, as the highest *A. caroliniana* tissue gold concentration was found in the 4-nm AuNP, DOC−, and R+ treatment and the lowest tissue gold concentrations were found in the DOC− and DOC+ R− treatment.

Organic Matter Interactions. Further evaluating these factors, it is important to note that aquatic plants are typically found in shallow, high productivity, eutrophic water systems high in natural organic matter. Investigating the interactions between AuNP sizes and dissolved organic carbon, it was found through TEM characterization that the 4-nm AuNPs associated with DOC in the highest numbers followed by the 18-nm AuNPs. Interestingly, it was found that the 30-nm AuNPs did not associate closely with the DOC (Figure 3).

Comparing the size measurements of the 4-nm AuNPs in the DOC− (10.0 ± 5.0-nm) and DOC+ (5.6 ± 1.8-nm) treatments, results indicate that the presence of DOC reduces particle core aggregation after 24 h. Even though the particle core aggregation is reduced, the DOC/AuNP complex becomes much larger than individual AuNPs as seen in Figure 3. In the 18-nm AuNP treatment, comparing the size range in the DOC− (23.3 ± 12.5-nm) and DOC+ (18.4 ± 8.4-nm) treatments, a reduction in particle polydispersity (Figure 1) and average particle core size is observed. However, due to high polydispersity in the DOC− treatments for both particle sizes, results are not statistically different. In the 30-nm AuNP treatment, comparing the size range in the DOC− (39.1 ± 8.0-nm) and DOC+ (42.3 ± 8.3-nm) treatments shows that the addition of DOC did not coincide with a decrease in average AuNP core diameter.

It has been observed that the presence of NOM can reduce particle aggregation by sterically hindering particle−particle interactions as a result of pH change, increased ionic strength, or from the presence of divalent cations, all causing a decrease in particle stability.[28−30] The absorption of compounds by organic matter is not uncommon. Organic matter is composed of various aliphatic and aromatic components that give rise to hydrophobic and hydrophilic regions. Organic matter primarily consists of polysaccharides and peptides as well as fulvic and humic acids that are derived from the breakdown of plant material and microbial degradation products.[19] Organic matter has been shown to act as a chelator reducing toxicity of metal ions and pesticides. Organic matter has also been shown to decrease the toxicity of silver nanoparticles to bacteria.[31] Also, organic matter is a known chelator of organic molecules, altering the toxicity and bioavailability of many pesticides.[32,33] The DOC/AuNP complex that is formed is hypothesized to be responsible for the decreased tissue gold concentrations observed.

Mechanism of Tissue Concentration Reduction. The presence of DOC reduced the bioavailability of the 4-nm AuNPs nearly 4-fold in *A. caroliniana* (Figure 2). For *A. caroliniana*, the presence of DOC mitigated AuNP size effect on tissue gold concentration. Hence, the presence of DOC drastically reduced the ability of the 4-nm AuNPs to be absorbed due to the increased size of the AuNP/DOC complex (Figure 3). The surface adsorption of AuNPs was expected, as indicated by the presence of gold in all species, but the significant decrease that results from the addition of DOC to the *A. caroliniana* treatment further supports decreased AuNP absorption. Although the significant effect of the DOC+ treatment resulted in the largest change in tissue gold concentration for the 4-nm *A. caroliniana* treatments, the

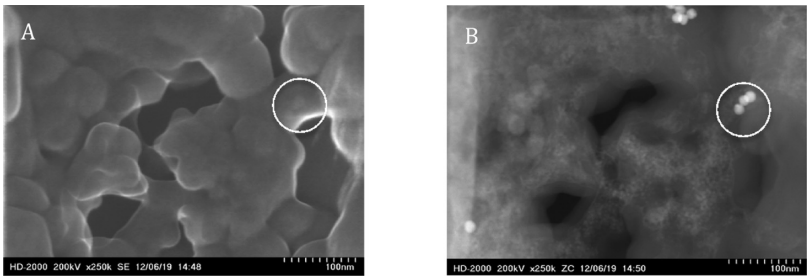

Figure 5. Micrographs (A) and (B) were taken of 18-nm gold nanoparticles exposed to Suwannee River dissolved organic matter in the same sample and location using two microscopy techniques. (A) Represents scanning electron microscopy and (B) shows elemental contrast microscopy. (A) Shows dimensional structure of dissolved organic matter, encapsulating the 18-nm gold nanoparticles as indicated by the circle. (B) Shows the elemental contrast of the same area, showing the gold nanoparticles within the dissolved organic matter. Note that images are superimposable and indicate the DOC/AuNP complex is much larger than individual particles.

overall trend in the DOC+ treatments indicated a reduced tissue gold concentration for each treatment.

Figure 4 shows a high-resolution electron micrograph detailing the surface interaction 18-nm AuNPs have in the DOC+ treatment. Note that the presence of organic carbon is closely intact to the AuNP core surface. Supporting this interaction, Figure 5 indicates that the DOC completely encapsulates the AuNPs. Using STEM microscopy, the same sample was observed under scanning electron and elemental contrast microscopy simultaneously. AuNPs were present and visible as white structures within the DOC+ treatment using elemental contrast; however, under scanning electron microscopy, observing only the surface, the AuNPs are observed covered in a layer of DOC (Figure 5). The formation of this larger complex of AuNPs and DOC resulted in decreased tissue concentrations due to the complex being too large for absorption.

These results indicate that AuNPs do interact with aquatic plants and bioaccumulate in the tissues. This bioaccumulation is affected not only by water quality parameters, such as ionic strength, hardness, and pH, but also by the presence of natural organic matter. The absorption of AuNPs is species specific and is dependent on the presence of roots for *A. caroliniana*. In any case, significant gold tissue concentrations for all treatments were found. Regardless of absorption, the need for ecotoxicity and transport studies of NMs in the aquatic environment exists. The mechanism of uptake, factors that influence the bioavailability, and the potential for trophic transfer of AuNPs in and potentially out of the aquatic ecosystem still need more attention.

AUTHOR INFORMATION

Corresponding Author

*E-mail: jbglenn@clemson.edu; phone: 864-646-2196; fax: 864-646-2277.

Notes

The authors declare no competing financial interest.

ACKNOWLEDGMENTS

The authors acknowledge the generous support of the Clemson University Public Service Activities, technical contribution number 6163 of the Clemson University Experiment Station, Dr. JoAn Hudson and Donald Mulwee at the Clemson Electron Microscope Facility, and also Norman Ellis for ICP/MS expertise. This research received financial support from Grants R833886, R834092, and R834575 from the U.S. Environmental Protection Agency's Science to Achieve Results (STAR) program. In addition, special thanks are extended to the anonymous reviewers for their comments and valuable contributions.

REFERENCES

(1) Ray, P. C.; Yu, H.; Fu, P. P. Toxicity and environmental risks of nanomaterials: Challenges and future needs. *J. Environ. Sci. Health, Part C* **2009**, *27*, 1−35.

(2) Klaine, S. J.; Alvarez, P. J. J.; Batley, G. E; Fernandes, T. F.; Handy, R. D.; Lyon, D. Y.; Mahendra, S.; McLaughlin, M. J.; Lead, J. R. Nanomaterials in the environment: Behavior, fate, bioavailability, and effects. *Environ. Toxicol. Chem.* **2008**, *27*, 1825−1851.

(3) Handy, R. D.; Owen, R.; Valsami-Jones, E. The ecotoxicology of nanoparticles and nanomaterials: Current status, knowledge gaps, challenges, and future needs. *Ecotoxicology* **2008**, *17*, 315−325.

(4) Klaine, S. J.; Koelmans, A. A.; Horne, N.; Carley, S.; Handy, R. D.; Kapustka, L.; Nowack, B.; von der Kammer, F. Paradigms to assess the environmental impacts of manufactured nanomaterials. *Environ. Toxicol. Chem.* **2012**, *31*, 3−14.

(5) Scown, T. M.; van Aerle, R.; Tyler, C. R. Review: Do engineered nanoparticles pose a significant threat to the aquatic environment? *Crit. Rev. Toxicol.* **2010**, *40*, 653−670.

(6) Peralta-Videa, J. R.; Zhao, L.; Lopez-Moreno, M. L.; de la Rosa, G.; Hong, J.; Gardea-Torresdey, J. L. Nanomaterials and the environment: A review for the biennium 2008−2010. *J. Hazard. Mater.* **2011**, *186*, 1−15.

(7) Nowack, B.; Ranville, J. F.; Diamon, S.; Gallego-Urrea, J. A.; Metcalfe, C.; Rose, J.; Horne, N.; Koelmans, A. A.; Klaine, S. J. Potential scenarios for nanomaterials release and subsequent alteration in the environment. *Environ. Toxicol. Chem.* **2012**, *31*, 50−59.

(8) Gottschalk, F.; Nowack, B. The release of engineered nanomaterials to the environment. *J. Environ. Monit.* **2011**, *13*, 1145−1155.

(9) Colvin, V. L. The potential environmental impact of engineered nanomaterials. *Nat. Biotechnol.* **2003**, *23*, 1166−1170.

(10) Limbach, L. K.; Bereiter, R.; Muller, E.; Krebs, R.; Galli, R.; Stark, W. J. Removal of oxide nanoparticles in a model wastewater treatment plant: Influence of agglomeration and surfactants on clearing efficiency. *Environ. Sci. Technol.* **2008**, *42*, 5828−5833.

(11) Gottschalk, F.; Sonderer, T.; Scholz, R. W.; Nowack, B. Modeled environmental concentrations of engineered nanomaterials (TiO_2, ZnO, Ag, CNT, Fullerenes) for different regions. *Environ. Sci. Technol.* **2009**, *43*, 9216−9222.

(12) Lee, W. M.; An, Y. J.; Yoon, H.; Kweon, H. S. Toxicity and bioavailability of copper nanoparticles to the terrestrial plants mung bean (*Phaseolus radiatus*) and wheat (*Triticum aestivum*): Plant agar test for water-insoluble nanoparticles. *Environ. Toxicol. Chem.* **2008**, *27*, 1915−1921.

(13) Larue, C.; Laurette, J.; Herlin-Boime, N.; Khodja, H.; Fayard, B.; Flank, A. M.; Brisset, F.; Carriere, M. Accumulation, translocation and impact of TiO_2 nanoparticles in wheat (*Titicum aestivum* spp.):

Influene of diameter and crystal phase. *Sci. Total Environ.* **2012**, *431*, 197−208.
(14) Corredor, E.; Testillano, P. S.; Coronado, M. J.; Gonzalez-Melendi, P.; Fernandez-Pacheco, R.; Marquina, C.; Ibarra, M. R.; de la Fuente, J. M.; Rubiales, D.; Perez-de-Luque.; Risueno, M. C. Nanoparticle penetration and transport in living pumpkin plants: In situ subcellular identification. *BMC Plant Biol.* **2009**, *9*, 45.
(15) Zhu, H.; Han, J.; Xiao, J. Q.; Jin, Y. Uptake, translocation, and accumulation of manufactured iron oxide nanoparticles by pumpkin plants. *J. Environ. Monit.* **2008**, *10*, 713−717.
(16) Sabo-Attwood, T.; Unrine, J. M.; Stone, J. W.; Murphy, C. J.; Ghoshroy, S.; Blom, D.; Bertsch, P. M.; Newman, L. A. Uptake, distribution and toxicity of gold nanoparticles in tobacco (*Nicotiana xanthi*) seedlings. *Nanotoxicology* **2011**, *6*, 353−360.
(17) Lin, S.; Reppert, J.; Hu, Q.; Hudson, J. S.; Reid, M. L.; Ratnikova, T. A.; Rao, A. M.; Luo, H.; Ke, P. C. Uptake, translocation, and transmission of carbon nanomaterials in rice plants. *Small* **2009**, *5*, 1128−1132.
(18) Glenn, J. B.; White, S. A.; Klaine, S. J. Interactions of gold nanoparticles with aquatic macrophytes are size and species dependent. *Environ. Toxicol. Chem.* **2012**, *31*, 194−201.
(19) Navarro, E.; Baun, A.; Behra, R.; Hartmann, N. B.; Filser, J.; Miao, A. J.; Quigg, A.; Santschi, P. H.; Sigg, L. Environmental behavior and ecotoxicity of engineered nanoparticles to algae, plants, and fungi. *Ecotoxicology* **2008**, *17*, 372−386.
(20) Rico, C. M.; Majumdar, S.; Duarte-Gardea, M.; Peralta-Videa, J. R.; Gardea-Torresdey, J. L. Interaction of nanoparticles with edible plants and their possible implications in the food chain. *J. Agric. Food Chem.* **2011**, *59*, 3485−3498.
(21) Miralles, P.; Church, T. L.; Harris, A. T. Toxicity, uptake, and translocation of engineered nanomaterials in vascular plants. *Environ. Sci. Technol.* **2012**, *46*, 9224−9239.
(22) Kim, B.; Park, C. S.; Murayama, M.; Hochella, M. F. Discovery and characterization of silver sulfide nanoparticles in finial sewage sludge products. *Environ. Sci. Technol.* **2010**, *44*, 7509−7514.
(23) Kiser, M. A.; Westerhoff, P.; Benn, T.; Wang, Y.; Perez-Rivera, J.; Hristovski, K. Titanium nanomaterial removal and release from wastewater treatment plants. *Environ. Sci. Technol.* **2009**, *43*, 6757−6763.
(24) Denny, P. Sites of nutrient absorption in aquatic macrophytes. *J. Ecol.* **1972**, *60*, 819−829.
(25) Carpita, N.; Sabularse, D.; Montezinos, D.; Delmer, D. P. Determination of the pore size of cell walls of living plants cells. *Science* **1979**, *205*, 1144−1147.
(26) Judy, J. D.; Unrine, J. M.; Rao, W.; Wirick, S.; Bertsch, P. M. Bioavailability of gold nanoparticles to plants: Importance of particle size and surface coating. *Environ. Sci. Technol.* **2012**, *46*, 8467−8474.
(27) Dietz, K. J.; Herth, S. Plant nanotoxicology. *Trends Plant Sci.* **2011**, *16*, 582−589.
(28) Stankus, D. P.; Lohse, S. E.; Hutchison, J. E.; Nason, J. A. Interactions between natural organic matter and gold nanoparticles stabilized with different organic capping agents. *Environ. Sci. Technol.* **2011**, *45*, 3238−3244.
(29) Diegoli, S.; Manciulea, A. L.; Begum, S.; Jones, I. P.; Lead, J. R.; Preece, J. A. Interactions between manufactured gold nanoparticles and naturally occurring organic macromolecules. *Sci. Total Environ.* **2008**, *402*, 51−61.
(30) Nason, J. A.; McDowell, S. A.; Callahan, T. W. Effects of natural organic matter type and concentration on the aggregation of citrate-stabilized gold nanoparticles. *J. Environ. Monit.* **2012**, *14*, 1885−1892.
(31) Fabrega, J.; Fawcett, S. R.; Renshaw, J. C.; Lead, J. R. Silver nanoparticle impact on bacterial growth: Effect of pH, concentration, and organic matter. *Environ. Sci. Technol.* **2009**, *43*, 7285−7290.
(32) Haitzer, M.; Hoss, S.; Traunspurger, W.; Steinberg, C. Effects of dissolved organic matter (DOM) on the bioconcentration of organic chemicals in aquatic organisms. *Chemosphere* **1998**, *37*, 1335−1362.
(33) Deschauer, H.; Kogel-Knabner, I. Binding of a herbicide to water-soluble soil humic substances. *Sci. Total Environ.* **1992**, *117*, 393−401.
(34) Kelly, K. L.; Coronado, E.; Zhao, L. L.; Schatz, G. C. The optical properties of metal nanoparticles: The influence of size, shape, and dielectric environment. *J. Phys. Chem. B* **2003**, *107*, 668−677.
(35) Murphy, C. J.; Sau, T. K.; Gole, A. M.; Orendorff, C. J.; Gao, J.; Gou, L.; Hunyadi, S. E.; Li, T. Anisotropic metal nanoparticles: Synthesis, assembly, and optical applications. *J. Phys. Chem. B* **2005**, *109*, 13857−13870.
(36) Murphy, C. J.; Gole, A. M.; Hunyadi, S. E.; Stone, J. W.; Sisco, P. N.; Alkilany, A.; Kinard, B. E.; Hankins, P. Chemical sensing and imaging with metallic nanorods. *Chem. Commun.* **2008**, 544−557.
(37) Murphy, C. J.; Gole, A. M.; Stone, J. W.; Sisco, P. N.; Alkilany, A. M.; Goldsmith, E. C.; Baxter, S. C. Gold nanoparticles in biology: Beyond toxicity to cellular imaging. *Acc. Chem. Res.* **2008**, *41*, 1721−1730.
(38) Barrena, R.; Casals, E.; Colon, J.; Font, X.; Sanchez, A.; Puntes, V. Evaluation of the ecotoxicity of model nanoparticles. *Chemosphere* **2009**, *75*, 850−857.
(39) Turkevich, J.; Stevenson, P. C.; Hillier, J. A study of the nucleation and growth processes in the synthesis of colloidal gold. *J. Discuss. Faraday Soc.* **1951**, *11*, 55−75.
(40) Fren, G. Preparation of gold dispersions of varying particle size: Controlled nucleation for the regulation of the particle size in monodisperse gold suspensions. *Nat. Phys. Sci.* **1973**, *241*, 20−22.
(41) Anderson, C.; Moreno, F.; Geurts, F.; Wreesmann, C.; Ghomshei, M.; Meech, J. A comparative analysis of gold-rich plant material using various analytical methods. *Microchem. J.* **2005**, *81*, 81−85.
(42) Kurepa, J.; Paunesku, T.; Vogt, S.; Arora, H.; Rabatic, B. M.; Lu, J.; Wanzer, M. B.; Woloschak, G. E.; Smalle, J. A. Uptake and distribution of ultrasmall anatase TiO_2 alizarin red S nanoconjugates in *Arabidopsis thaliana*. *Nano Lett.* **2010**, *10*, 2296−2302.
(43) Lin, D.; Xing, B. Root uptake and toxicity of ZnO nanoparticles. *Environ. Sci. Technol.* **2008**, *42*, 5580−5585.
(44) Birbaum, K.; Brogioli, R.; Scellenberg, M.; Martinoia, E.; Stark, W. J.; Gunther, D.; Limbach, L. K. No evidence for cerium dioxide nanoparticle translocation in maize plants. *Environ. Sci. Technol.* **2010**, *44*, 8718−8723.
(45) Busby, C. H.; Gunning, B. E. S. Microtubules and morphogenesis in stomata of the water fern Azolla: An unusual mode of guard cell and pore development. *Protoplasm* **1984**, *122*, 108−119.
(46) Haramoto, T.; Ikusima, I. Life cycle of *Egeria densa* planch., an aquatic plant naturalized in Japan. *Aquat. Bot.* **1988**, *30*, 389−403.